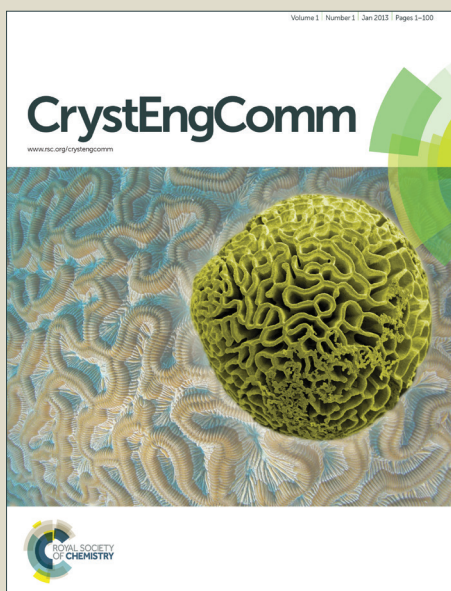


CrystEngComm

Accepted Manuscript



This is an *Accepted Manuscript*, which has been through the Royal Society of Chemistry peer review process and has been accepted for publication.

Accepted Manuscripts are published online shortly after acceptance, before technical editing, formatting and proof reading. Using this free service, authors can make their results available to the community, in citable form, before we publish the edited article. We will replace this *Accepted Manuscript* with the edited and formatted *Advance Article* as soon as it is available.

You can find more information about *Accepted Manuscripts* in the [Information for Authors](#).

Please note that technical editing may introduce minor changes to the text and/or graphics, which may alter content. The journal's standard [Terms & Conditions](#) and the [Ethical guidelines](#) still apply. In no event shall the Royal Society of Chemistry be held responsible for any errors or omissions in this *Accepted Manuscript* or any consequences arising from the use of any information it contains.

Cite this: DOI: 10.1039/c0xx00000x

www.rsc.org/xxxxxx

ARTICLE TYPE

Flying Upconversion Fluorescent Particles and Direct Observation of Energy transfer and Depopulation Processes

Kezhi Zheng, Weiping Qin*, Guanshi Qin, Dan Zhao, and Changfeng Wu

5 Received (in XXX, XXX) Xth XXXXXXXXX 201X, Accepted Xth XXXXXXXXX 201X

DOI: 10.1039/b000000x

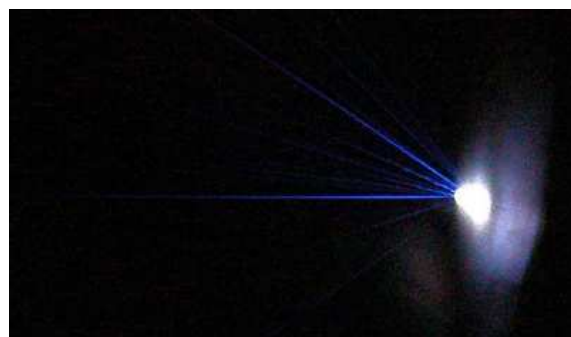
Flying particles with visible fluorescence were observed when a target, $\text{ZnF}_2:\text{Tm}^{3+}/\text{Yb}^{3+}$, was irradiated by a pulsed infrared laser of 953.6 nm. Narrow blue beams showed the particles ejecting with upconversion emissions. The changing brightness along fluorescence traces exhibited the energy transfer from Yb^{3+} ions to Tm^{3+} ions and the depopulation of excited Tm^{3+} ions. Parameters of micro-explosions induced by the pulsed laser were estimated by analyzing these flying particles. Comparing with the target, these particles have strong ability of infrared-to-ultraviolet upconversion. These results not only suggest a way to explore micro-explosions induced by pulsed lasers but also provide a feasible scheme for developing ultraviolet upconversion materials.

15 Introduction

Pulsed laser deposition (PLD) is a useful technique in developing novel materials.¹⁻⁵ When an intense pulsed laser is focused onto a target, instantaneous explosions (deposition) will occur on its surface. Significant material removal occurs in the form of luminous plasma plumes and ejecting fragments (particles) of the target as soon as the energy density of the pulsed laser exceeds a threshold. According to literatures,^{2,6-8} atoms, ions and particles in the plume-like plasma eject from the focus spot at high speed, faster than 10^4 meters per second in vacuum. The plasma matter is usually collected on a substrate to form a new optoelectronic material. However, up to now, few researchers have paid attention to the flight behaviors of the ejecting fragments in PLD, not only because the PLD particles are in the sizes of micro-scale but also because they move too fast to be observed. Here, we present an observation of the high-speed particles in PLD with an optical method. By employing an upconversion (UC) target and a near infrared (NIR) pulsed laser, we observed the particles flying with UC fluorescence against a dark background and found that they exhibited various flight behaviors. By analyzing the fluorescence traces and flight behaviors of the flying particles, not only the energy transfer between Yb^{3+} and Tm^{3+} ions and the depopulation of excited states of Tm^{3+} ions were investigated intuitively, but also some parameters of micro-explosions were calculated demonstratedly.

As we know, compared with oxides, hydroxides, and chlorides *etc*, fluorides with good stability and low phonon energy are considered as more suitable host materials for investigating upconversion luminescence.⁹⁻¹¹ The former made them possible host materials to investigate their upconversion luminescence properties, the latter would decrease the nonradiative relaxation

process during the UC population and improve the upconversion luminescence properties greatly. In this work, ZnF_2 was chosen as host material because of its high melting point, good phase stability, and low phonon energy.



50 **FIG. 1** Under the bombardment of 953.6 nm pulsed laser, fling particles of $\text{ZnF}_2: 10\%\text{Yb}^{3+}, 0.2\%\text{Tm}^{3+}$ with bright UC emissions lined straight fluorescence traces.

Experimental procedures

55 The target, polycrystalline $\text{ZnF}_2: 10\%\text{Yb}^{3+}, 0.2\%\text{Tm}^{3+}$, was prepared by high-temperature solid state reaction method. All chemicals were of analytical grade and used without further purification. ZnF_2 (99.9%) was supplied by Beijing Fine Chemical Company and YbF_3 (99.9%), and TmF_3 (99.9%) were supplied by Yutai Qingda Chemical Technology Co., Ltd. China. All components according to the compositions in molar fraction were mixed uniform by using agate mortar. Subsequently, the mixture was reacted in an electric furnace using aluminium oxide

crucibles at 1000°C for 1 h. A gentle flow of argon gas was used throughout the solid state reaction. Laser depositions were performed with an excited Raman laser that has been described in Ref. 12. Its second Stokes line was at 953.6 nm with the pulse energy of ~10 mJ. At room temperature and in air atmosphere, the NIR laser was focused onto the surface of ZnF₂:Yb³⁺, Tm³⁺ target using a convex lens with a focal length of 15 cm, and the focused spot was about 2 μm in diameter.

Results and discussion

XRD analysis confirmed that the target sample is pure ZnF₂, which is in good agreement with the standard value for the ZnF₂ (JCPDS No.71-1971) (see ESI, Fig. S1).

While blue and red UC fluorescence emitted, thin, straight, bright, blue beams streamed out of the target surface, as shown in Fig. 1, which was photographed with a CCD camera. The ejected beams were fluorescence traces lined by flying particles with UC luminescence of Tm³⁺ ions. According to our observation, the lengths of some bright beams could reach 20-30 cm. As depicted in Fig. 1, blue beams are spurting out of the target (bright white) under the bombardment of pulsed NIR laser. The brightness along the blue traces shows the intensities of the UC fluorescence from the moving particles. The brightest point of a fluorescence trace is generally in the middle. The changing intensity along the fluorescence trace reflects the immigrating processes of excitation energy. This optical phenomenon can be explained as below: Pulsed NIR laser caused micro-explosions on the surface of the target. When the target's fragments were exploded off the surface, the pulsed NIR laser excited them simultaneously. Meanwhile, Yb³⁺ ions in these fragments absorbed NIR photons of 953.6 nm, resulting in the electron excited to the ²F_{5/2} level from ground state ²F_{7/2} and then transferred the energy to Tm³⁺ ions, as shown in Fig. 2.¹³⁻¹⁶ When the Tm³⁺ ions populated at ¹I₆, ¹D₂, and ¹G₄ states de-excited to lower levels radiatively, these ejecting particles lined straight fluorescence traces. As a consequence, the fadein of the fluorescence traces exhibits the energy transfer process from Yb³⁺ to Tm³⁺, and the fadeout displays the de-excitation process of excited Tm³⁺ ions. Different processes may act in populating the higher excited states of Tm³⁺ ions in the Yb³⁺-Tm³⁺ codoped ZnF₂ under the NIR excitation. They include excited state absorption (ESA), cross relaxation resonant energy transfer (CRET), and energy transfer (ET) between Yb³⁺ and Tm³⁺.

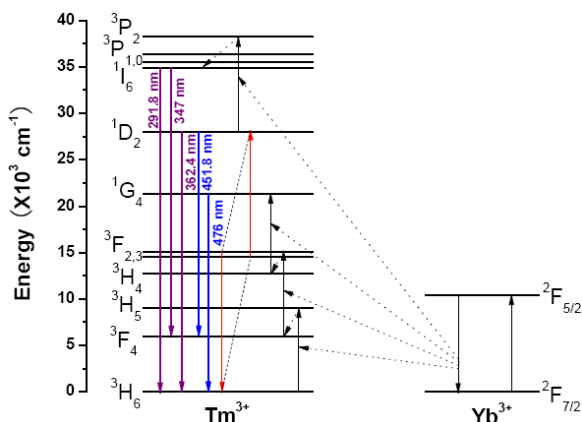


FIG. 2 Energy level diagrams of Yb³⁺ and Tm³⁺ ions in ZnF₂: 10%Yb³⁺, 0.2%Tm³⁺, and possible energy transfer, cross-relaxation and up-converted processes.

A digitized brightness curve on flight distance was drawn in Fig. 3(b) by measuring the brightness of the fluorescence trace in Fig. 3(a). The overscaled intensity near zero-distance point came from the intense fluorescence and plasma on the target surface. As a comparison, a temporal evolution curve of Tm³⁺ UC fluorescence of the collected particles is given in Fig. 3(c). It was measured with a boxcar integrator under the same pulsed NIR laser. There is a good correspondence between the two profiles except using different abscissas. In addition, the time constant for a micro-explosion is very short (less than a few nanoseconds).⁴ Therefore, it is reasonable to deduce that the flight time for the particle reaching at the brightest point is about 150 μs, as shown in Fig. 3(c). Furthermore, the flight speed of the particle in air can be estimated based on the accordance, and it was calculated at about 140 m/s. Such a speed is about two orders lower in magnitude than those in vacuum. This discrepancy may originate from the difference of ambient pressures in different experiments. If the interaction time of a pulse and the target is taken as 10 ns (pulse width) and the particle is treated as a sphere for advantageous estimation, the pressure induced by the micro-explosion can be roughly estimated at ~2.3 GPa for a 5 μm particle.²¹ If we take account of the influence from the air, the pressure of the micro-explosion should be much higher than the estimation. On all accounts, it is an effective method in investigating micro-explosions induced by pulsed lasers.

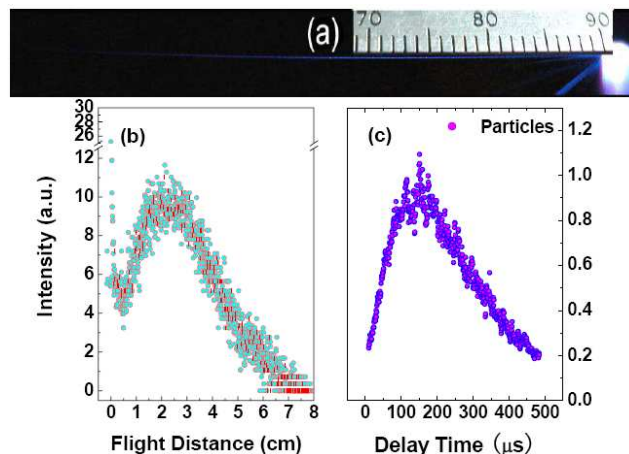


FIG. 3 (a) a long fluorescence trace and a ruler were photographed at the same distance; (b) the digitized brightness of the fluorescence trace changed with flight distance; (c) the temporal evolution curve of collected particles obtained with a boxcar integrator. (b) and (c) get their maximum at ~2.0 cm and ~150 μs, respectively.

Some detailed information about the ejected fragments also can be obtained by studying these flying particles. Several flight states (or behaviors) and a ruler photographed at the same distance, as well as the digitized brightness curves of these fluorescent traces, are given in Fig. 4. From the long fluorescence trace in Fig. 4(a), 140 m/s flight speed has been calculated. Fig. 4(b) is a short fluorescence trace and the corresponding brightness was digitized in Fig. 4(f). The short trace suggests a slow flight speed only about 30 m/s and a lower explosion pressure (about 0.5 GPa). Fig. 4(c) and 4(d) are dashed beam traces, which indicate a periodic change of brightness along each

fluorescence trace. More details can be seen from Fig. 4(i), which is the amplified photograph of Fig. 4(d). Fig. 4(g) and 4(h) are two digitized brightness curves taken from Fig. 4(c) and 4(d), respectively. They suggest that there was a spin motion around each centroid of moving particles. According to the periods, we calculated their spin frequencies to be 40,000 Hz for the beam in Fig. 4(c) and 55,000 Hz for the beam in Fig. 4(d), respectively.

Fig. 4(e) shows two fluorescence spots rotating on two interlaced spiral courses. When we magnify Fig. 4(e), a red spring-like trace can be clearly seen, as shown in Fig. 4(j). The red fluorescence came from the transition of Tm^{3+} ($^1\text{G}_4 \rightarrow ^3\text{F}_4$, 645 nm). This red spring-like trace confirms further the rotational movement of flying particles.

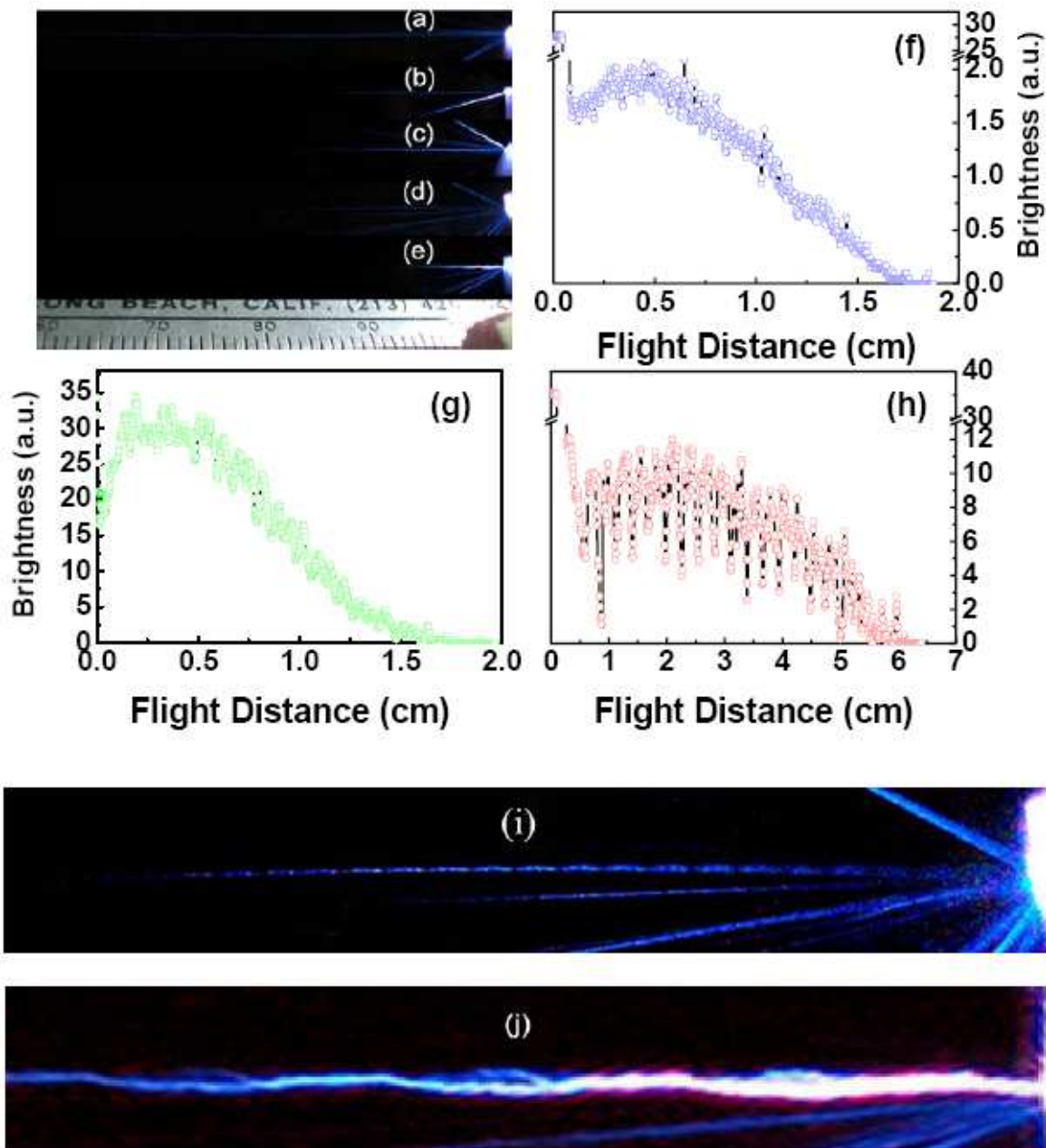


FIG. 4 Different flight behaviors and a ruler photographed at the same distance. (a) is a long fluorescence trace; (b) is a short fluorescence trace; (c) and (d) are dashed traces. (e) shows a spiral flight behavior. (f) – (h) are the digitized brightness curves taken from (b) – (d) traces, respectively. (i) is the magnified photograph of (d) trace, which suggests a spin motion. (j) is the magnified photograph of (e) trace, which shows a red spring-like flight route. The spring-like trace indicates a rotational motion.

In order to study the optical properties of the flying particles, we collected them in a thin polyvinyl butyral (PVB) layer on a glass slice by putting the glass slice in flight ways and facing the PVB layer to the target. The PLD particles attached to the PVB layer when the micro-explosions occurred. Some particles retained their fluorescence for a while after they located in the PVB layer. Collected particles were investigated by using a scanning electron microscope (SEM), and most particle sizes lie in a range of hundreds of nanometers to microns, as shown in the inset of Figure 5.

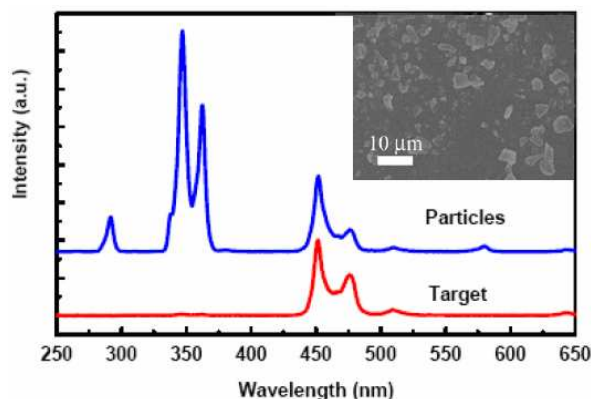


FIG. 5 Upconversion spectra of the particles and the target under the excitation of 980 nm laser diode. The inset is the corresponding SEM image of the collected particles.

The spectrum of the collected particles was recorded with a spectrometer (Hitachi-4500). When a diode laser of 980 nm with 1 Watt output was focused on the particles by an object lens ($\times 20$), strong UC light could be seen easily with naked eye. At room temperature, we recorded the UC spectra of the particles and the target, respectively. There is a significant difference between them, as shown in Fig. 5. After normalizing the spectra with the emission at 451.8 nm ($^1D_2 \rightarrow ^3F_4$), we can find a strong 362.4 nm emission ($^1D_2 \rightarrow ^3H_6$), a much more intense 347 nm emission ($^1I_6 \rightarrow ^3F_4$) and a weak 291.8 nm emission ($^1I_6 \rightarrow ^3H_6$) in the spectrum of the PLD particles. In comparison with the target, the PLD particles have much stronger ability of emitting UV UC fluorescence under the identical NIR excitation. The changed branching ratio of $^1D_2 \rightarrow ^3F_4$ and $^1D_2 \rightarrow ^3H_6$ transitions reveals that some new metastable structures have formed in the PLD particles.^{12,22-23} The twisted lattice structures were induced by the intense interaction between light and matter. The blue emission at 451.8 nm and the UV emission at 362.4 nm were produced by 4-photon UC process and the UV emissions 347 nm and 291.8 nm by 5-photon UC process.²⁴⁻²⁶

Conclusions

In conclusion, with a pulsed laser of 953.6 nm, flying particles of $ZnF_2:Tm^{3+}/Yb^{3+}$ in PLD were investigated on their flight behaviors and optical properties. Some parameters about the micro-explosions induced by the pulsed laser were estimated through analyzing the fluorescence traces of PLD particles. In these flight behaviors, spin motions with tens of thousands Hz and spiral motions with interlaced courses were found. The

process of energy transfer from Yb^{3+} ion to Tm^{3+} ion was observed directly from the fluorescence traces for the first time.

Acknowledgments

This work was supported by the National Natural Science Foundation of China (NNSFC) (grants 11274139, and 61275189), China Postdoctoral Science Foundation (2012M520668). The authors would like to thank Prof. Shihua Huang for his offering the digitization program and helpful discussions.

Notes and references

State Key Laboratory on Integrated Optoelectronics, College of Electronic Science and Engineering, Jilin University, Changchun 130012, China. Fax: +86-431-85168241-8325; Tel: +86-431-85153853; E-mail: wqjin@jlu.edu.cn.

- 1 C. B. Juang, H. Cai, M. F. Becker, J. W. Keto, and J. R. Brock, *Appl. Phys. Lett.* 1994, **65**, 40.
- 2 D. H. Lowndes, D. B. Geohegan, A. A. Puretzky, D. P. Norton, and C. M. Rouleau, *Science* 1996, **273**, 898.
- 3 A. M. Morales and C. M. Lieber, *Science* 1998, **279**, 208.
- 4 P. R. Willmott and J. R. Huber, *Rev. Mod. Phys.* 2000, **72**, 315.
- 5 S. Y. Chen and P. Shen, *Phys. Rev. Lett.* 2002, **89**, 096106.
- 6 D. W. Koopman and R. R. Goforth, *Phys. Fluids* 1974, **17**, 1560.
- 7 D. B. Geohegan and A. A. Puretzky, *Appl. Surf. Sci.* 1996, **96**, 131.
- 8 R. F. Wood, J. N. Leboeuf, D. B. Geohegan, A. A. Puretzky, and K. R. Chen, *Phys. Rev. B* 1998, **58**, 1533.
- 9 F. Vetrone, R. Naccache, V. Mahalingam, C. G. Morgan, and J. A. Capobianco, *Adv. Funct. Mater.* 2009, **19**, 2924.
- 10 X. F. Wang, Y. Y. Bu, Y. Xiao, C. X. Kan, D. Lu, and X. H. Yan, *J. Mater. Chem. C* 2013, **1**, 3158.
- 11 Y. S. Liu, D. T. Tu, H. M. Zhu, R. F. Li, W. Q. Luo, and X. Y. Chen, *Adv. Mater.* 2010, **22**, 3266.
- 12 W. P. Qin, G. S. Qin, Y. H. Chung, Y. I. Lee, C. D. Kim, and K. W. Jang, *J. Kor. Phys. Soc.* 2004, **44**, 925.
- 13 F. Auzel, *Proc. IEEE* 1973, **61**, 758.
- 14 F. Auzel, P. Pecile, and D. Morin, *J. Electrochem. Soc.* 1975, **122**, 101.
- 15 O. L. Malta, P. A. Santa-Cruz, G. F. De Sã, and F. Auzel, *J. Solid State Chem.* 1987, **68**, 314.
- 16 R. J. Thrash, L.F. Johnson, *J. Opt. Soc. Am. B* 1994, **11**, 881.
- 17 B. Dong, H. W. Song, H. Q. Y, H. Zhang, R. F. Qin, X. Bai, G. H. Pan, S. Z. Lu, F. Wang, L. B. Fan, and Q. L. Dai, *J. Phys. Chem. C* 2008, **112**, 1435.
- 18 G. J. De, W. P. Qin, J. S. Zhang, J. S. Zhang, Y. Wang, C. Y. Cao, and Y. Cui, *J. Lumin.* 2007, **122**, 128.
- 19 X. F. Wang, J. Zheng, Y. Xuan, and X. H. Yan, *Opt. Express* 2013, **21**, 21596.
- 20 S. Heer, K. Kompe, H. U. Güdel, and M. Haase, *Adv. Mater.* 2004, **16**, 2102.
- 21 The force acting on a particle can be expressed as $F = m\Delta v/\Delta t$; where $m = \rho V$ is the mass of the particle; Δv the change of velocity; Δt the interacting time; ρ the density; V the volume of the particle. The density (ρ) of the sample is $4.943 \times 10^3 \text{ kg/m}^3$. If the particle is treated as a sphere with a diameter of 5 μm , $m = 3.2 \times 10^{-13} \text{ kg}$, $F = 4.3 \times 10^{-3} \text{ N}$, the pressure $p = F/S = 2.3 \text{ GPa}$; where S is the interacting area.
- 22 S. Tanabe, K. Tamai, K. Hirao, and N. Soga, *Phys. Rev. B* 1996, **53**, 8358.
- 23 G. F. Wang, W. P. Qin, J. S. Zhang, J. S. Zhang, Y. Wang, C. Y. Cao, L. Wang, G. D. Wei, P. F. Zhu, and R. Z. Kim, *J. Phys. Chem. C* 2008, **112**, 12161.
- 24 Z. Q. Li, C. L. Li, Y. Y. Mei, L. M. Wang, G. H. Du, and Y. J. Xiong,

